within experimental error as those from the corresponding $5\alpha,3\beta$-hydroxy steroids. Thus the EI and CAD spectra provide a nearly complete identification of the unknown molecular structure, including C-3 and C-5 (but not C-17) stereochemistry.

Obviously the structural predictions from the EI spectrum greatly reduced the number of CAD reference spectra which had to be measured to obtain matches with those from the unknown. The presence of the complementary $84^+/234^+$ pair also simplified the identification. By "Stevenson's rule" such product ions resulting from the same dissociation, and thus competing for the charge, will have similar abundances only if they have similar ionization energies. For example, in the EI spectra of steroids **1–4** the homologous complementary ion $C_5H_{10}O^+\cdot$ ($m/z$ 86) is of low abundance, compromising identification of that part of the molecule. A possible solution is the proposed CAD structure determination of neutral products of ionic reactions.[28] Complementary pairs of even-electron ions formed from the molecular ion can also be useful, as shown in a separate study of fentanyl derivatives.[29] For production of both complementary ions of an even-electron ion pair, chemical ionization can also help; even if $AB^+ \rightarrow A^+ + B\cdot$, not $\rightarrow A\cdot + B^+$, it is possible that $HAB^+ \rightarrow HA + B^+$.[24,30] Other molecular ion adducts produced by CI or chemical derivatization of the molecule[1,2] might also provide other types of fragment ions whose CAD spectra will be structurally useful.

## Conclusion

Structure determination by MS/MS should be most applicable to the types of molecules for which EI mass spectra are most useful. The extra dimension of structural information from the secondary CAD spectra can provide specific fragmentation pathway and substructural identification, which will be particularly valuable for larger and more complex molecules, as well as those only available in quantities too low for techniques such as nuclear magnetic resonance.

## Experimental Section

CAD and MI mass spectra were measured on an MS/MS instrument utilizing a double-focusing Hitachi RMH-2 as MS-I, a He molecular beam to produce CAD, and an electrostatic analyzer as MS-II,[28] using an ion source temperature of 130 °C, ion accelerating potential of 9.8 KV, and a collision gas pressure giving a precursor ion transmittance of 25%. Each CAD spectrum is the computer average of at least 20 scans.

Compounds **1–7, 10**, and **13** were purchased from Sigma Chemical Co., and cyclopropyl methyl ketone and 3-penten-2-one from Aldrich Chemical Co. Compounds **8, 9**, and **11** were made from **10**, and **12** from **13** by standard methods, the products giving the expected proton NMR and EI mass spectra.

**Registry No.** **1**, 566-58-5; **2**, 566-56-3; **3**, 80-92-2; **4**, 80-90-0; **5**, 516-95-0; **6**, 80-97-7; **7**, 516-92-7; **8**, 4352-06-1; **9**, 566-65-4; **10**, 516-59-6; **11**, 14778-11-1; **12**, 848-62-4; **13**, 516-55-2; cyclopropylmethyl-carbinol, 2566-44-1; 3-penten-2-ol, 1569-50-2; 1-penten-4-ol, 625-31-0; acetylcyclopropane, 765-43-5; 2-penten-4-one, 625-33-2; 1-penten-4-one, 13891-87-7.

(28) McLafferty, F. W.; Todd, P. J.; McGilvery, D. C.; Baldwin, M. A. *J. Am. Chem. Soc.* **1980**, *102*, 3360–3363.

(29) Cheng, M. T.; Kruppa, G. H.; McLafferty, F. W.; Cooper, D. A. *Anal. Chem.* **1982**, *54*, 2204.

(30) Field, F. H. In "Mass Spectrometry"; Maccoll, A., Ed.; Butterworths: London, 1972; Chapter 5.

# Intramolecular Electron Transfer in a Series of Mixed-Valence Copper(II)–Copper(I) Complexes

**Russell C. Long and David N. Hendrickson\***

*Contribution from the School of Chemical Sciences, University of Illinois, Urbana, Illinois 61801. Received July 19, 1982*

**Abstract:** A series of seven mixed-valence binuclear copper(II)–copper(I) complexes of macrocyclic ligands has been prepared to study systematically the factors affecting intramolecular electron transfer. The mixed-valence copper complexes are similar to the one prepared by Gagné et al.,[3b] except the methyl groups on the phenolic residue have been replaced by *tert*-butyl substituents. In addition, the diamine linkages B and B' have been varied in the molecule
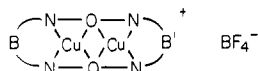


Four of the complexes have both copper sites equivalent with B = B' = propylene (I), 2,2-dimethylpropylene (II), butylene (III), or 2,2'-biphenylene (IV). Three of the complexes have two different copper sites: B = propylene, B' = 2,2-dimethylpropylene (V); B = propylene, B' = 2,2'-biphenylene (VI); and B = propylene, B' = butylene (VII). Chemical reduction of the binuclear copper(II) complexes with sodium dithionite was used to prepare the mixed-valence complexes. Each binuclear copper(II) complex exhibits two quasi-reversible one-electron reduction waves. Variable-temperature EPR data, taken for acetone solutions from room to liquid-nitrogen temperature, are presented. In the low-temperature glass medium, each species shows an EPR spectrum characteristic of the single unpaired electron localized on one copper center. At room temperature in solution, four of the molecules (I, II, III, and V) are EPR delocalized, whereas the other three molecules each show four-line copper hyperfine spectra. Approximate temperatures of conversion in solution from EPR localized to EPR delocalized are noted for several of the complexes. Intervalence transfer (IT) bands are seen in the electronic absorption spectra for the seven complexes.

Only a few mixed-valence binuclear $Cu^{II}Cu^{I}$ complexes have been reported. They are of importance in the study of intramolecular electron transfer[1] and as a model of the mixed-valence state detected for binuclear copper sites in cuproproteins.[2] Gagné and co-workers[3] reported the electrochemical preparation of a $Cu^{II}Cu^{I}$ complex with Robson's macrocyclic binucleating ligand. At room

(1) "Mixed-Valence Compounds, Theory and Applications in Chemistry, Physics, Geology, and Biology"; Brown, D. B., Ed.; Reidel Publishing Co.: Boston, 1980.

(2) Solomon, E. I., In "Copper Proteins"; Spiro, T. G., Ed.; Wiley: New York, 1981; Chapter 2 and references therein.

(3) (a) Gagné, R. R.; Koval, C. A.; Smith, T. J. *J. Am. Chem. Soc.* **1977**, *99*, 8367. (b) Gagné, R. R.; Koval, C. A.; Smith, T. J.; Cimolino, M. C. *Ibid.* **1979**, *101*, 4571. (c) Gagné, R. R.; Henling, L. M.; Kistenmacher, T. J. *Inorg. Chem.* **1980**, *19*, 1226.

temperature their mixed-valence $Cu^{II}Cu^{I}$ complex exhibited a seven-line EPR spectrum in solution, which indicates that the single unpaired electron is delocalized over the two copper centers ($I = \frac{3}{2}$) on the EPR time scale. In contrast, Addison[4] had earlier reported that the EPR spectrum for a related (methyl group on iminium carbons) binuclear mixed-valence $Cu^{II}Cu^{I}$ complex invariably exhibits a four-line copper hyperfine pattern at room temperature in solution. In this second case, the single unpaired electron is clearly localized on one copper ion on the EPR time scale.

The goal of the present study was to prepare a series of mixed-valence binuclear $Cu^{II}Cu^{I}$ complexes to facilitate a systematic study of the factors that control the rate of intramolecular electron transfer. This goal was accomplished by first devising a means to prepare such a mixed-valence $Cu^{II}Cu^{I}$ complex chemically, not electrochemically. As illustrated below, $BF_4^-$ salts of seven different mixed-valence $Cu^{II}Cu^{I}$ complexes were prepared, four (I–IV) having both copper sites equivalent and three (V–VII) where the macrocyclic binucleating ligand has two inequivalent metal sites.
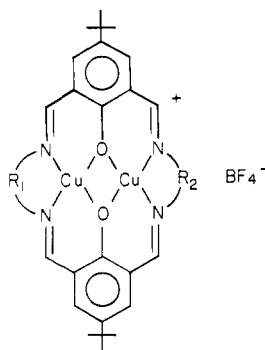
I, $R_1 = R_2$ = propylene
II, $R_1 = R_2$ = 2,2'-dimethylpropylene
III, $R_1 = R_2$ = butylene
IV, $R_1 = R_2$ = 2,2'-biphenylene
V, $R_1$ = propylene; $R_2$ = 2,2'-dimethylpropylene
VI, $R_1$ = propylene; $R_2$ = 2,2'-biphenylene
VII, $R_1$ = propylene; $R_2$ = butylene

## Results and Discussion

**Compound Preparation.** Tetrafluoroborate salts of the seven binuclear $Cu^{II}Cu^{II}$ complexes related to complexes I–VII were prepared in relatively straightforward procedures. The three $Cu^{II}Cu^{II}$ complexes that have two different coordination sites were prepared by first condensing 1 mol of diamine with 2 mol of diformylphenol and then adding a cupric salt. The resulting mononuclear $Cu^{II}$ complex was then condensed in a template fashion with 1 mol of a different diamine.

Chemical reduction of the binuclear copper(II) complexes with sodium dithionite was used to prepare the mixed-valence complexes I–VII. Two molar equivalents of a given binuclear $Cu^{II}Cu^{II}$ complex were dissolved in methanol in the presence of 4 equiv of NaOH. After this solution was degassed, 1 molar equiv of sodium dithionite dissolved in degassed water was added under argon by using Schlenkware techniques. The $BF_4^-$ salt of the mixed-valence $Cu^{II}Cu^{I}$ complex precipitated immediately upon addition of the dithionite solution. These mixed-valence complexes can be recrystallized to give microcrystalline samples. X-ray quality crystals were obtained for complex II, for example, by evaporation of a toluene–acetone solution in an inert atmosphere box. X-ray diffraction data were collected on these crystals, but a relatively large unit cell with two different binuclear units in the asymmetric unit and loss of the toluene molecules of crystallization during data collection led to the termination of structural work on this crystal system. Structural work continues, however.

**Electrochemistry of Binuclear $Cu^{II}Cu^{II}$ Complexes.** The diamines selected to prepare the above seven mixed-valence $Cu^{II}Cu^{I}$

(4) Addison, A. W. *Inorg. Nucl. Chem. Lett.* **1976**, *12*, 899.

Table I. Electrochemical Data for Binuclear $Cu^{II}Cu^{II}$ Complexes[a]

| $Cu^{II}Cu^{II}$ complex | $E_{1/2}^1$ | | | $E_{1/2}^2$ | | |
|---|---|---|---|---|---|---|
| | DP[b] | CV[c] | Δ[d] | DP[b] | CV[c] | Δ[d] |
| I | -0.538 | -0.530 | 0.072 | -0.932 | -0.922 | 0.073 |
| II | -0.557 | -0.554 | 0.067 | -0.948 | -0.942 | 0.107 |
| III | -0.336 | -0.332 | 0.080 | -0.810 | -0.810 | 0.074 |
| IV | -0.240 | -0.232 | 0.075 | -0.649 | -0.643 | 0.076 |
| V | -0.546 | -0.537 | 0.071 | -0.943 | -0.935 | 0.067 |
| VI | -0.381 | -0.375 | 0.075 | -0.833 | -0.824 | 0.075 |
| VII | -0.411 | -0.397 | 0.071 | -0.931 | -0.920 | 0.078 |

[a] $N,N$-Dimethylformamide (DMF) solution with 0.1 M tetrabutylammonium perchlorate electrolyte. All potentials are referenced to the normal hydrogen electrode (NHE). [b] Volts vs. NHE; scan rate = 2 mV/s; modulation amplitude = 10 mV; potentials are corrected for modulation amplitude. [c] Volts vs. NHE; scan rate = 10 mV/s. [d] Separation in volts between waves ($E_{ox} - E_{red}$) seen in cyclic voltammograms. Ferrocene dissolved in these solutions under the same conditions gave a Δ value of 0.070 V for the oxidation wave at 0.400 V vs. NHE.
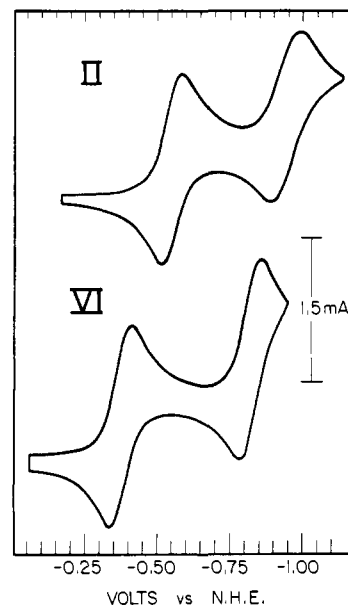


**Figure 1.** Cyclic voltammograms of binuclear $Cu^{II}Cu^{II}$ complexes II and VI in DMF. Two successive one-electron reduction waves are seen for each complex at a scan rate of 10 mV/s.

complexes and corresponding binuclear $Cu^{II}Cu^{II}$ species should produce considerable variation in the $N_2O_2$ copper coordination geometries. The 2,2'-biphenylene linkage in complex IV, for example, has a non-zero dihedral angle between the two phenyl moieties, and consequently the copper coordination geometry in this complex would be intermediate between square planar and tetrahedral. Electrochemical data should reflect these differences in coordination geometries.

The $Cu^{II}Cu^{II}$ analogues of complexes I–VII were examined in DMF with cyclic voltammetry and differential pulse polarography. Comparable concentrations of ferrocene were added for an internal check on redox potentials and reversibilities.[5] Electrochemical data are summarized in Table I and are illustrated in Figures 1 and 2. In each case the $Cu^{II}Cu^{II}$ complex can be reduced in two successive quasi-reversible one-electron waves. Cyclic voltammograms obtained for the $Cu^{II}Cu^{II}$ complexes II and VI appear in Figure 1. Reduction waves are seen at -0.375 and -0.824 V (vs. NHE) for complex VI at a platinum electrode with a 0.1 M TBAP electolyte. These waves seem to be fairly reversible even at a scan rate of 10mV/s. The *tert*-butyl substituents on our ligand increase the solubility of the complexes (particularly in the $Cu^{I}Cu^{I}$ form) relative to Gagné's complex, which has methyl substituents

(5) Gagné, R. R.; Koval, C. A.; Lisensky, G. C. *Inorg. Chem.* **1980**, *19*, 2855.

*Electron Transfer in Cu$^{II}$-Cu$^I$ Complexes*

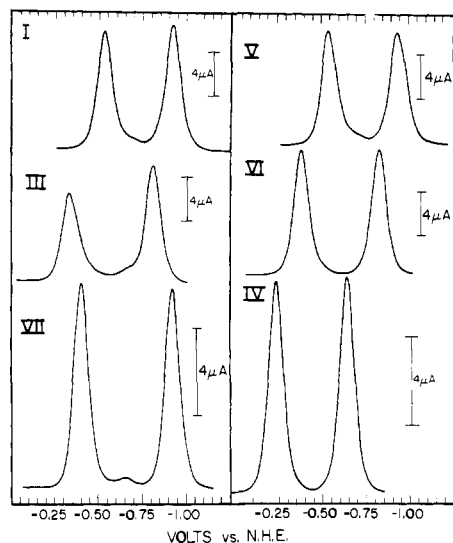*J. Am. Chem. Soc., Vol. 105, No. 6, 1983* 1515



**Figure 2.** Differential pulse voltammograms of six of the binuclear Cu$^{II}$Cu$^{II}$ complexes in DMF at a scan rate of 2 mV/s.

in place of the two *tert*-butyl substituents. Both of the reduction waves illustrated in Figure 1 for Cu$^{II}$Cu$^{II}$ complex VI have peak-to-peak separations of 0.075 V at a scan rate of 10mV/s. Ferrocene dissolved in this solution was found to show a peak-to-peak separation of 0.075 V for the oxidation wave at 0.40 V.

As can be seen in Table I, only the second reduction wave for complex II at −0.942 V showed an appreciable deviation in peak-to-peak wave separation relative to the 0.075-V ferrocene value. This complex apparently tends to dimerize in solution. Evidence for this was seen in the EPR experiments (vide infra).

It is of interest to note that in spite of the considerable variation in coordination geometries and in reduction potentials in the series, the separation in successive one-electron reduction waves does not vary appreciably from one complex to another (see Figure 2). The smallest wave separation ($E_1 − E_2 = 0.39$ V) is observed for complex II, whereas the largest (0.52 V) is observed for complex VII. Apparently the interaction of the electronic manifolds of the two copper ions in a given Cu$^{II}$Cu$^{II}$, Cu$^{II}$Cu$^I$, or Cu$^I$Cu$^I$ complex does not change much as the copper coordination geometry is changed in the series. There has been interest in understanding the separation in one-electron reduction potentials of binuclear Cu$^{II}$Cu$^{II}$ complexes.[3,6-8] In this regard it would be interesting to determine the variation in magnetic exchange interaction in the series of Cu$^{II}$Cu$^{II}$ complexes. The small change in wave separation from one complex to another leads to a relatively small range of conproportionation constants, $3.7 \times 10^6$ for complex II to $7.1 \times 10^8$ for complex VII. Conproportionation constants are listed in Table II.

The variation in reduction potentials observed for complexes I–IV is readily understood. Small differences ($\sim 0.02$ V) are seen between the reduction potentials for complexes I and II, as expected. The Cu$^{II}$Cu$^{II}$ complex III is easier to reduce than either complex I or II because the butylene linkage in complex III is more flexible than the propylene linkages in complexes I and II, and this permits a Cu$^I$ coordination geometry distorted somewhat toward tetrahedral. In this same vein we find that complex IV with 2,2′-biphenylene connectors is the complex that is most readily reduced.

The electrochemistry of Cu$^{II}$Cu$^{II}$ complexes V, VI, and VII is interesting, for each of these complexes has two different metal sites. Figure 2 illustrates differential pulse polarograms for two of these three asymmetric complexes. Complex V, which is related to complex I by addition of two methyl substituents to one of the

**Table II.** Conproportionation Constants[a]

| complex | $K_{con}$ |
|---------|-----------|
| I | $4.3 \times 10^6$ |
| II | $3.7 \times 10^6$ |
| III | $1.2 \times 10^8$ |
| IV | $9.0 \times 10^6$ |
| V | $5.2 \times 10^6$ |
| VI | $4.0 \times 10^7$ |
| VII | $7.1 \times 10^8$ |

[a] Conproportionation constants are calculated for the equilibrium

$$Cu^{II}Cu^{II}L^{2+} + Cu^ICu^IL \overset{K_{con}}{\rightleftharpoons} 2Cu^{II}Cu^IL^+$$
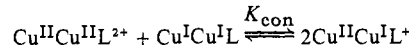
with the potentials for the two reduction waves as follows: $E^1 − E^2 = 0.0591 \log K_{con}$.

propylene groups of complex I, shows differential pulse reduction waves at −0.541 and −0.938 V. These two potentials are within 1–3 mV of the averages of the corresponding potentials for complexes I and II. Because the first wave reduction potentials for complexes I, II, and V span only 19 mV (16 mV for second wave), an analysis of differences is not called for.

More pronounced differences are present in the two coordination sites of complexes VI and VII. Figure 2 (right panel) illustrates how the two potentials of complex VI compare to those for the related complexes I (the potentials for complexes I and V are nearly equal) and IV. It was anticipated that the first electron added to the Cu$^{II}$Cu$^{II}$ form of complex VI would lead to a reduction of the copper ion in the biphenylene site. Naively, then, the first one-electron reduction wave for complex VI might have been expected at a potential of −0.235 V, the first potential for complex IV. Instead the first wave for complex VI is found at −0.376 V, which is only 8 mV more positive than the average of the first potentials for complexes I and IV. Similarly, the second wave for complex VI is only 42 mV more negative than the average of potentials for complexes I and IV. Several electronic and steric factors could be responsible for the fact that the two reduction potentials for complex VI are not simply the first and second potentials of complexes IV and I, respectively. Consider the first reduction potential for complex VI. The propylene linkage in the Cu$^{II}$Cu$^{II}$ form of complex VI could affect the dihedral angle at the biphenylene linkage and make the Cu$^{II}$ ion in this second site harder to reduce than for complex IV. Obviously the two Cu$^{II}$ ions in Cu$^{II}$Cu$^{II}$ complex VI are involved in an interaction that is propagated largely by the phenolic oxygen atoms (a magnetic exchange interaction). If this bonding interaction is strong, the molecular orbital of the Cu$^{II}$Cu$^{II}$ complex VI into which the first electron is added (i.e., LUMO) would consist of appreciable contributions from atomic orbitals centered on both Cu$^{II}$ ions. Such a strong electronic communication between the two Cu$^{II}$ ions would tend to give a reduction potential intermediate between those for the symmetric counterparts. More evidence about the nature of delocalization in the ground state of the mixed valence Cu$^{II}$Cu$^I$ species is available in the EPR results.

Complex VII also has intermediate reduction potentials. The first reduction potential is 26 mV more positive than the average of the first potentials of I and III, whereas the second potential is 55 mV more negative than the average. With the limited amount of data available, it is tempting to say that the electronic communication is strong in complexes V–VII and potentials close to averages are observed. Steric effects would modify this view. For example, one diamine moiety could affect the conformation at the second diamine in the Cu$^{II}$Cu$^{II}$ complex. In addition, after the first electron is added, the copper coordination geometries in the formally Cu$^{II}$Cu$^I$ species could be changed from those in the original Cu$^{II}$Cu$^{II}$ complex.

**EPR for Cu$^{II}$Cu$^I$ Complexes.** EPR spectra were run for all seven mixed-valence Cu$^{II}$Cu$^I$ complexes dissolved in three different solvents: CH$_2$Cl$_2$, acetone, and a 3:2 mixture of acetone and toluene. Spectra were run at various temperatures from room to liquid-nitrogen temperature. In solution at room temperature, complexes I–III and V show an isotropic pattern with seven copper

(6) Patterson, G. S.; Holm, R. H. *Bioinorg. Chem.* **1975**, *4*, 257.

(7) Hasty, E. F.; Wilson, L. J.; Hendrickson, D. N. *Inorg. Chem.* **1978**, *17*, 1834.

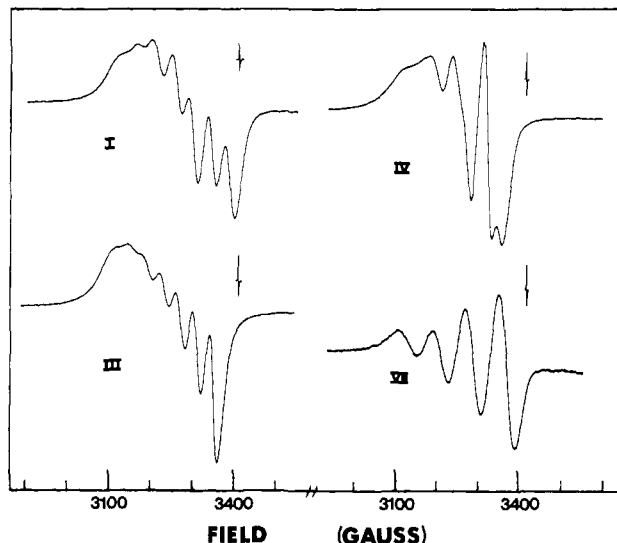(8) Fenton, D. E.; Schroeder, R. R.; Lintvedt, R. L. *J. Am. Chem. Soc.* **1978**, *100*, 1931.

1516 *J. Am. Chem. Soc., Vol. 105, No. 6, 1983*

*Long and Hendrickson*

**Figure 3.** Room-temperature X-band EPR spectra for toluene–acetone (3:2) solutions of mixed-valence $Cu^{II}Cu^{I}$ complexes I, III, IV, and VII. The small sharp signal superimposed above each spectrum is that for a DPPH standard.

**Table III.** X-Band EPR Parameters[a]

| complex | T, K | $g_\perp$[b] | $g_{av}$[c] | $g_\parallel$[b] | $A_\parallel$,[d] $10^{-4}$ cm$^{-1}$ | $A_{av}$,[d] $10^{-4}$ cm$^{-1}$ |
|---------|------|---------|---------|---------|------|------|
| I | 298 | | 2.088 | | | 41 |
| | 100 | 2.06 | | 2.24 | 193 | |
| II | 298 | | 2.104 | | | 41 |
| | 100 | 2.06 | | 2.23 | 194 | |
| III | 298 | | 2.102 | | | 37 |
| | 100 | 2.06 | | 2.23 | 184 | |
| IV | 298 | | 2.116 | | | 64 |
| | 100 | 2.06 | | 2.24 | 174 | |
| V | 298 | | 2.090 | | | 41 |
| | 100 | 2.06 | | 2.23 | 194 | |
| VI | 298 | | 2.105 | | | 78 |
| | 100 | 2.06 | | 2.23 | 187 | |
| VII | 298 | | 2.107 | | | 82 |
| | 100 | 2.06 | | 2.23 | 191 | |

[a] EPR spectra were run for toluene–acetone (3:2) solutions. Values of $g_{av}$ and $A_{av}$(Cu) were taken from room-temperature spectra, whereas values of $g_\perp$, $g_\parallel$, and $A_\parallel$ were determined by simulating the frozen glass spectra taken at ~100 K. [b] Estimated error of ±0.01. [c] Estimated error of ±0.002. [d] Estimated error of ±1 × $10^{-4}$ cm$^{-1}$.

hyperfine lines. Figure 3 gives representative spectra for complexes I and III in acetone and data appear in Table III. It is clear that the slight asymmetry present in complex V is not sufficient to localize the unpaired electron on the EPR time scale at room temperature. From the seven-line patterns it is found that complexes I, II, and V have average copper hyperfine splittings ($A_{av}$) of 41 (1) × $10^{-4}$ cm$^{-1}$. The butylene complex III has an $A_{av}$ value of 37 (1) × $10^{-4}$ cm$^{-1}$. The average copper hyperfine splitting ($A_{av}$) for an EPR-delocalized species is expected to be approximately one-half that found for the EPR-localized $Cu^{II}Cu^{I}$ binuclear mixed-valence complex. These four mixed-valence complexes are delocalized on the EPR time scale at room temperature. It was surprising to find that the room-temperature solution spectra for complexes IV, VI, and VII are characteristic of species that are localized on the EPR time scale. Four-line hyperfine patterns are seen for these three complexes with average copper hyperfine splittings of 64 (1) × $10^{-4}$ cm$^{-1}$, 78 (1) × $10^{-4}$ cm$^{-1}$, and 82 (1) × $10^{-4}$ cm$^{-1}$, respectively. A four-line pattern was what Addison[4] found for his mixed-valence $Cu^{II}Cu^{I}$ complex. On the other hand, Gagné et al.[3] reported a seven-line pattern ($A$ = 41.77 × $10^{-4}$ cm$^{-1}$ in acetone) for their $Cu^{II}Cu^{I}$ complex at room temperature in solution. It is relevant to note that changing the *tert*-butyl substituents on complex I to methyl substituents gives Gagné's
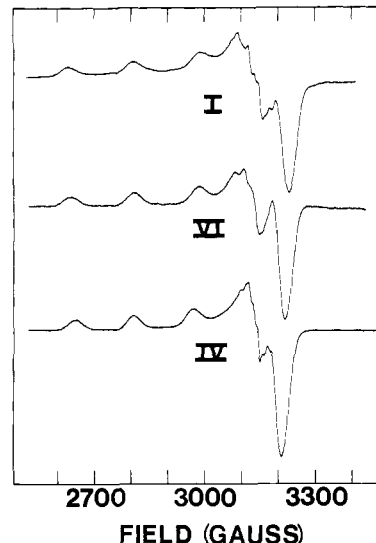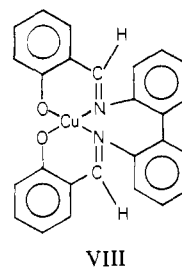
complex. In short, it is clear from the room-temperature spectra in Figure 3 that the intramolecular electron-transfer rate in solution is quite responsive to changes in the binucleating ligand.

In a frozen (105 K) glass of acetone–toluene (3:2), all seven of the mixed-valence $Cu^{II}Cu^{I}$ complexes exhibit "axial" spectra with four-line copper hyperfine impressed on the $g_\parallel$ signal. Spectra are shown in Figures 4 and 5 (Figure 5 is in the supplementary material), and EPR parameters are found in Table III. In a frozen glass, the unpaired electron in each of the seven complexes is localized on one of the two copper ions on the EPR time scale. The asymmetric complexes VI and VII each have two appreciably different copper centers. Careful examination of the frozen glass spectra for complexes VI and VII indicates at which of the two different copper sites the unpaired electron is localized.

Complexes I and IV are the symmetric counterparts of asymmetric complex VI. The copper hyperfine splitting ($A_\parallel$) on the $g_\parallel$ signal is found to be 193 (1) × $10^{-4}$ cm$^{-1}$ for complex I in a frozen glass and 174 (1) × $10^{-4}$ cm$^{-1}$ for complex IV. Presumably the smaller value of $A_\parallel$ for complex IV reflects a copper coordination geometry distorted from square planar toward tetrahedral, a result of the biphenylene linkages. Larin et al.[9] reported the EPR data for complex VIII, which is obviously a "monomeric"



**Figure 4.** Frozen (105 K) acetone–toluene (3:2) glass X-band EPR spectra for mixed-valence $Cu^{II}Cu^{I}$ complexes I, IV, and VI.



VIII

analogue of complex IV. They reported an $A_{av}$ value of 65.45 (2) × $10^{-4}$ cm$^{-1}$ ($g_{av}$ = 2.124 (4)) for complex VIII in toluene, and in a glass, $A_\parallel$(Cu) was found to be 178.8 (2) × $10^{-4}$ cm$^{-1}$. The X-ray structure[10] of this monomeric complex indicates a copper coordination geometry intermediate between square planar and tetrahedral with the dihedral angle between the two metallocycles set at 37°.

The frozen glass spectrum for asymmetric complex VI is compared with those observed for complexes I and IV in Figure 4. The $A_\parallel$ value for complex VI is 187 (1) × $10^{-4}$ cm$^{-1}$, which suggests that the unpaired electron is localized on the propyl-

(9) Larin, G. M.; Kolosov, V. A.; Vikulova, N. K.; Panova, G. V. *Zh. Neorg. Khim.* **1974**, *19*, 1873.

(10) Cheeseman, T. P.; Hall, D.; Waters, T. N. *J. Chem. Soc. A* **1966**, 1396.
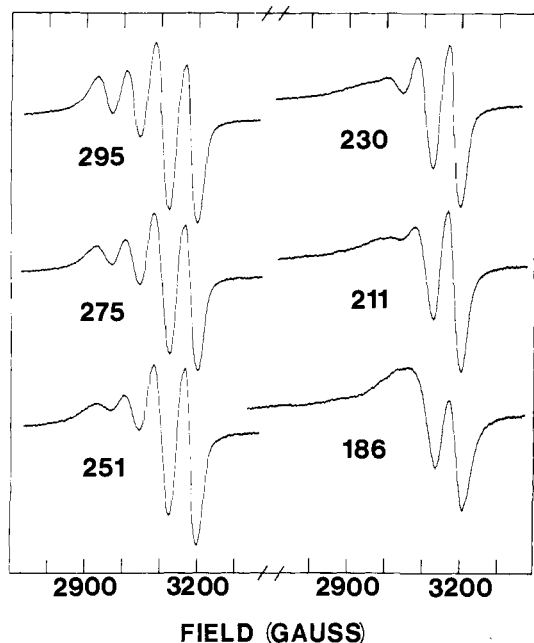
*Electron Transfer in Cu$^{II}$-Cu$^I$ Complexes*

*J. Am. Chem. Soc., Vol. 105, No. 6, 1983* 1517



**FIELD (GAUSS)**

**Figure 6.** Variable-temperature X-band EPR spectra for mixed-valence Cu$^{II}$Cu$^I$ complex VII in acetone.



**FIELD (GAUSS)**

**Figure 7.** Variable-temperature X-band EPR spectra for mixed-valence Cu$^{II}$Cu$^I$ complex I in acetone.

ene-copper site, not the biphenylene-copper site. That is, the 187 (1) × 10$^{-4}$ cm$^{-1}$ $A_{\parallel}$ value is much closer to the 193 (1) × 10$^{-4}$ cm$^{-1}$ $A_{\parallel}$ value found for the propylene complex I than the 174 (1) × 10$^{-4}$ cm$^{-1}$ $A_{\parallel}$ value found for the biphenylene complex IV. It remains to explain why the first and, for that matter, the second reduction potentials observed for complex VI are close to the averages of those found for complexes I and IV. There is the distinct possibility that compared to the species in solution, the molecular dimensions and conformation of mixed-valence complex VI experience some small but important changes when a solution is frozen or a solid crystallizes.

The frozen glass spectrum for asymmetric complex VII is plotted together with those for complexes II and III in Figure 5. The spectrum for complex II shows more noise than the other two because it was necessary to study this complex at a lower concentration. Complex II exhibits the greatest tendency to dimerize in solution at higher concentrations. Additional EPR signals are seen that are characteristic of such a triplet-state dimer (vide infra). The $A_{\parallel}$(Cu) values observed for complexes I, III, and the asymmetric species VII are 193 (1) × 10$^{-4}$ cm, 184 (1) × 10$^{-4}$ cm$^{-1}$, and 191 (1) × 10$^{-4}$ cm$^{-1}$, respectively. It appears that the unpaired electron is again localized on the propylene-copper site in complex VII, as expected.

Perhaps the most important results in this study can be gleaned from the variable-temperature solution EPR spectra for the seven mixed-valence species. Some of the large amount of data of this type that we have collected for these compounds appears in Figures 6–10. At the outset it should be mentioned that several factors potentially affect these dilute solution-state spectra. Certainly the most important are the nature of the molecular tumbling in solution, $g$ tensor anisotropy, and intramolecular electron transfer. It is a near to impossible task at best to simulate these solution-state spectra. However, it is possible to identify an approximate temperature at which a given mixed-valence species converts in solution between EPR-localized and EPR-delocalized states.

Variable-temperature (295–186 K) EPR spectra for complex VII in acetone are given in Figure 6. Similar results were obtained for the other two mixed-valence species that are also localized in solution at room temperature, namely, complexes IV and VI. The spectra in Figure 6 illustrate the influence of the rate of molecular tumbling upon the appearance of the spectrum. Since complex VII is already localized at ~295 K, lowering the temperature of the solution only leads to a slower rate of molecular tumbling in solution. It is obvious that even at 295 K complex VII is too bulky to tumble in solution fast enough to give a complete averaging
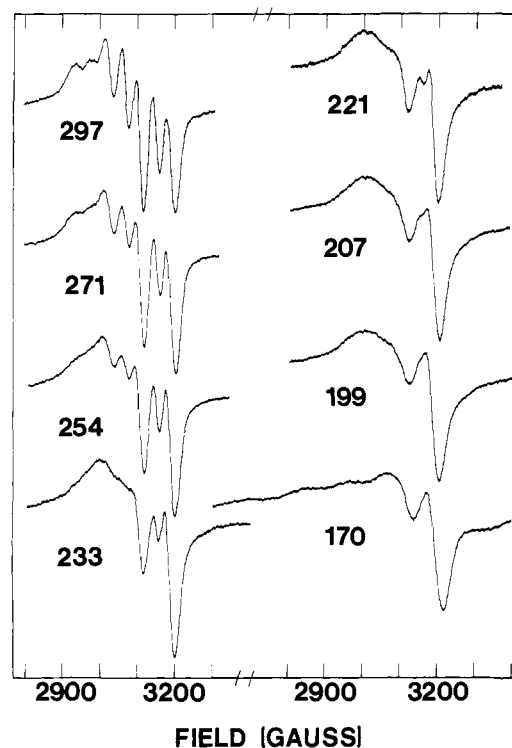
of the $g$ and $A$ tensors. The four lines that are seen do not have the same line width. At increasingly lower temperatures the localized mixed-valence molecules tumble at slower rates. Two of the low-field components of the four-line pattern have become so broadened by ~230 K that they cannot be resolved. Recall that acetone freezes at 187.8 K. Below this temperature both $g_{\parallel}$ and $g_{\perp}$ signals are seen, as illustrated in Figure 5. The spectral patterns seen in Figure 6 serve as a guide of what to expect for an EPR-localized species.

The variable-temperature EPR behavior of the symmetric mixed-valence propylene complex I is summarized in Figure 7. At 297 K, this complex is delocalized on the EPR time scale. Even at temperatures down to ~220–230 K, the complex appears to be delocalized, as evidenced by the copper hyperfine splitting that is seen. The transformation temperature from a delocalized to a localized description is ~200 K. By temperatures of ~170 K, there is the first sign of the copper hyperfine on the $g_{\parallel}$ signal. The temperature dependence that is exhibited by complex I is very similar (same coalescence temperature) to that observed by Gagné and co-workers.[3] This is reasonable because their complex also has propylene diamines condensed to diformylphenols.

An appreciably different transformation temperature is found for the butylene mixed-valence complex III. Close inspection of the spectra in Figure 8 sets the transformation temperature at ~250 K for this complex. It is clear that there are copper hyperfine splittings characteristic of an EPR-delocalized species present in the 261 K spectrum, whereas the 246 K spectrum is very similar in appearance to the 230–250 K spectra observed for the localized complex VII (see Figure 6).

EPR data for the two dimethylpropylene complexes, V and II, given in Figures 9 and 10 (Figure 10 is in the supplementary material). At the same concentration used in the EPR experiments for the other five Cu$^{II}$Cu$^I$ binuclear complexes these two complexes tend to dimerize at low temperatures in solution. A tendency to dimerize was also noted for Gagné's Cu$^{II}$Cu$^I$ species at low temperatures in solution. Apparently the *tert*-butyl substituents help several of our complexes avoid this complication. When two molecules of complex II associate, the two doublet states ($S = {}^1/_2$) interact to give one singlet ($S = 0$) and one triplet ($S = 1$) state. Zero-field splitting is seen for the EPR-active triplet state of the dimer. For these complexes the fingerprint for this zero-field
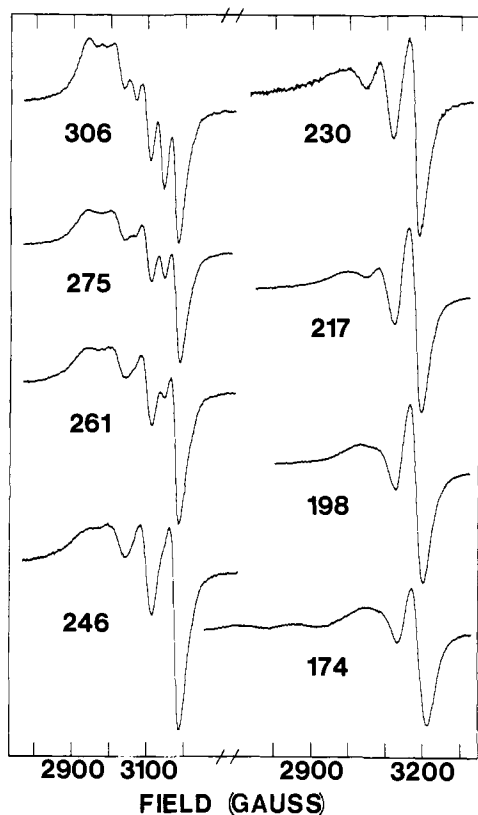
**Figure 8.** Variable-temperature X-band EPR spectra for mixed-valence Cu$^{II}$Cu$^{I}$ complex III in acetone.



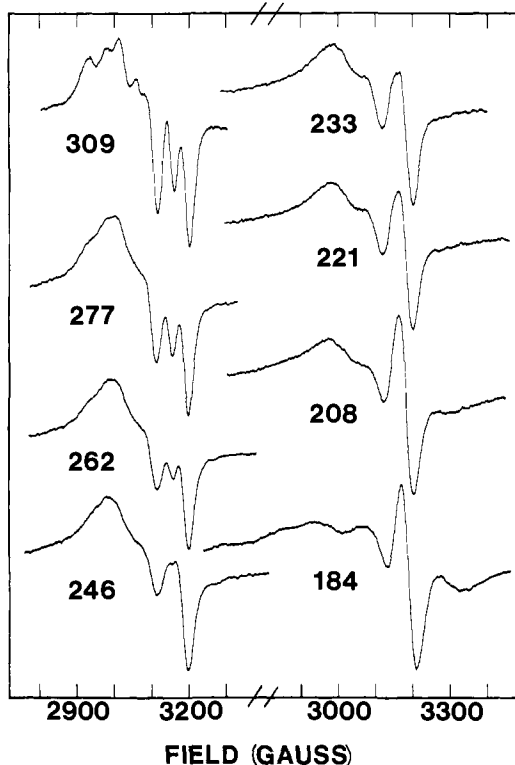**Figure 9.** Variable-temperature X-band EPR spectra for mixed-valence Cu$^{II}$Cu$^{I}$ complex V in acetone.

splitting is seen in the presence of a new feature at ~3340 C ($g$ = 1.96). Such a high-field signal at $g$ = 1.96 is not appropriate for a doublet-state copper species. It is of interest to note as well that the liquid-helium temperature EPR spectra for *solid samples* of mixed-valence complexes II and V also show this same high-field signal, as can be seen in Figure 11. These two complexes are
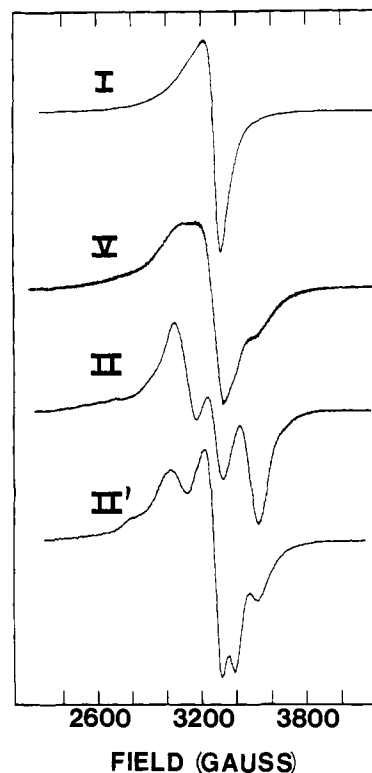


**Figure 11.** Liquid-helium-temperature X-band EPR spectra for solid samples of the BF$_4^-$ salt mixed-valence complexes I, II, and V and for a solid sample of the BPh$_4^-$ salt of the cation in complex II.

dimerized in the solid state. The tracing marked II' in Figure 11 is the spectrum for a solid sample of the BPh$_4^-$ salt of the mixed-valence cation in complex II. The BPh$_4^-$ counterion usually leads to better magnetic dilution in the solid state compared to the BF$_4^-$ ion.

In spite of the problems with complexes II and V, it is still possible to estimate from the EPR spectra in Figures 9 and 10 that the transformation temperature for both of these complexes is ~230 K.

The temperature dependencies of the EPR spectra for complexes IV, VI, and VII were examined from room temperature up to 390 K. Only small spectral changes were noted. There are no signs of either mixed-valence species converting from EPR localized to EPR delocalized as the temperature of the acetone solution was increased to 390 K.

Estimates of the activation energy ($E_{th}^*$) for intramolecular electron transfer can be made from the variable-temperature EPR data for mixed-valence complexes I–VII. Following Gagné's lead, $k_{th}$ is taken to be equal to the EPR lifetime (5.5 × 10$^8$ s$^{-1}$) at the coalescence temperature for each compound. A unit transmission coefficient corresponding to adiabatic electron transfer is assumed. A value for $E_{th}^*$ can then be calculated with the equation

$$k_{th} = \frac{kT}{h} e^{-E_{th}^*/RT}$$

where the symbols have their usual meanings. For example, in the case of the butylene complex III, the transformation temperature from EPR delocalized to EPR localized was found to be ~250 K, which together with $k_{th}$ = 5.5 × 10$^8$ s$^{-1}$ gives an $E_{th}^*$ value of 4.6 kcal/mol. Complexes IV, VI, and VII remain EPR localized in solution even up to 390 K. In these three cases $E_{th}^*$ is calculated to be greater than 7.4 kcal/mol. Table IV summarizes the transformation temperatures and $E_{th}^*$ values for the whole series of complexes. In addition, values for $k_{th}$ calculated at 298 K with the assumption that $E_{th}^*$ does not change in the given temperature range are given in Table IV. If all of the above assumptions are valid, it can be seen that the intramolecular thermal electron-transfer rate at room temperature varies in this series of complexes from less than 2.2 × 10$^7$ s$^{-1}$ to 1.6 × 10$^{10}$ s$^{-1}$.

*Electron Transfer in Cu^{II}-Cu^{I} Complexes*

*J. Am. Chem. Soc., Vol. 105, No. 6, 1983* 1519

Table IV. Intramolecular Electron-Transfer Parameters[a]

| complex | EPR coalescence temperature, K | $E_{th}^{\ddagger,b}$ kcal/mol | $k_{th}$(298 K), s$^{-1}$ |
|---|---|---|---|
| I | 200 | 3.6 | $1.6 \times 10^{10}$ |
| II | 230 | 4.2 | $5.6 \times 10^9$ |
| III | 250 | 4.6 | $2.9 \times 10^9$ |
| IV | >390 | >7.4 | $<2.2 \times 10^7$ |
| V | 230 | 4.2 | $5.6 \times 10^9$ |
| VI | >390 | >7.4 | $<2.2 \times 10^7$ |
| VII | >390 | >7.4 | $<2.2 \times 10^7$ |

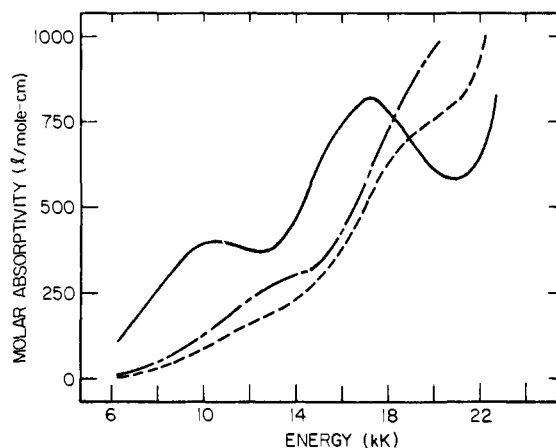[a] See text for details of assumptions made.   [b] Activation energy.



**Figure 12.** Electronic absorption spectra at room temperature for mixed-valence Cu$^{II}$Cu$^{I}$ complexes I (—), III (---), and VII (- - -) in acetone.

**Electronic Absorption Spectra.** The intervalence transfer (IT) band is a particularly characteristic feature generally present in the near-IR region of the electronic absorption spectrum for a mixed-valence complex.[11,12] Piepho, Krausz and Schatz[13] (PKS) recently developed a virbonic coupling model for mixed-valence compounds. From the band contours of the IT band, zeroth, first, and second moments can be determined. With such a determination it is then possible to calculate the electronic and vibronic coupling factors for a given mixed-valence complex. Unfortunately, at present the PKS theory has only been extended to mixed-valence complexes with high molecular symmetry. Because the mixed-valence Cu$^{II}$Cu$^{I}$ complexes I–VII likely have relatively low symmetry, the PKS theory cannot be used to analyze their IT bands. However, it is interesting to examine the electronic absorption spectra of these complexes to see if there are any qualitative trends in position and intensity of IT bands.

The near-IR and visible regions of the electronic absorption spectra of five of our mixed-valence complexes dissolved in acetone are illustrated in Figures 12 and 13. The spectra for complexes II and V are very similar to the spectrum observed for complex I, see Table V. As can be seen in Figure 12, complex I shows an IT band at 10.5 kK with a molar extinction coefficient ($\epsilon$) of 401 M$^{-1}$ cm$^{-1}$. This band is not found in the spectrum for an acetone solution of the corresponding Cu$^{II}$Cu$^{II}$ complex (see Table IV). Gagné et al.[3] reported an IT band at 10.0 $\times$ 10$^3$ cm$^{-1}$ with $\epsilon$ 480 M$^{-1}$ cm$^{-1}$ for their mixed-valence Cu$^{II}$Cu$^{I}$ complex. A d–d band is also seen at 17.1 $\times$ 10$^3$ cm$^{-1}$ for complex I. This band has enhanced intensity ($\epsilon$ 818 M$^{-1}$ cm$^{-1}$) compared to the same d–d band (17.0 $\times$ 10$^3$ cm$^{-1}$, $\epsilon$ 109 M$^{-1}$ cm$^{-1}$) observed for the corresponding Cu$^{II}$Cu$^{II}$ complex.

The spectrum for complex III is given in Figure 12. A poorly resolved band is observed at 13.5 kK, which possibly is the IT band for the butylene complex III. Regardless of this assignment, it is clear from Figure 12 that compared to the situation for complex
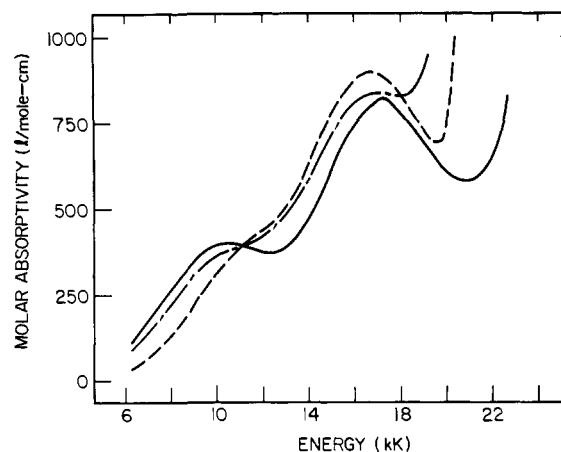
(11) Allen, G. C.; Hush, N. S. *Prog. Inorg. Chem.* **1967**, *8*, 257. Hush, N. *Ibid.* **1967**, *8*, 391.
(12) Robin, M. B.; Day, P. *Adv. Inorg. Chem. Radiochem.* **1967**, *10*, 247.
(13) Wong, K. Y.; Schatz, P. N. *Prog. Inorg. Chem.* **1981**, *28*, 369.



**Figure 13.** Electronic absorption spectra at room temperature for mixed-valence Cu$^{II}$Cu$^{I}$ complexes I (—), IV (- - -), and VI (- - - -) in acetone.

Table V. Electronic Absorption Spectral Data for Mixed-Valence Cu$^{II}$Cu$^{I}$L$^+$ and Cu$^{II}$Cu$^{II}$L$^{2+}$ Species

| complex | $\bar{v}$, kK ($\epsilon$, M$^{-1}$ cm$^{-1}$) acetone | CH$_2$Cl$_2$ |
|---|---|---|
| | Mixed-Valence Cu$^{II}$Cu$^{I}$L$^+$ | |
| I | 10.5 (401), 17.1 (818) | 5.8 (310), 8.6 (430), 17.2 (705) |
| II | 10.5 (355), 17.0 (632) | |
| III | sh 13.5 (303) | 13.4 (280) |
| IV | 10.7 (378), 16.8 (834) | 10.1 (280), 15.8 (570) |
| V | 10.5 (363), 17.1 (683) | |
| VI | sh 12.1 (189), 16.7 (896) | |
| VII | sh 12.6 (176), sh 19.4 (725) | |
| | Cu$^{II}$Cu$^{II}$L$^{2+}$ Complexes | |
| I | sh 14.6 (87), 17.0 (109) | |
| II | sh 15.9 (112), 17.3 (128) | |
| III | 13.2 (136), 15.6 (103) | |
| IV | 12.9 (215), 16.3 (168) | |
| VI | 13.7 (124), sh 16.2 (126), 17.0 (130) | |
| VII | 14.5 (97), 16.8 (123) | |

I, the IT band for complex III have moved to higher energy and, more importantly, has lost intensity. The reduced intensity of the IT band for complex III compared to complex I is in keeping with the EPR results for these complexes. Complex III was seen to have a higher temperature EPR transformation temperature (250 K) than complex I (200 K). Thus, complex III has a larger $E_{th}^{\ddagger}$ than complex I (4.6 vs. 3.6 kcal, respectively). If the vibronic coupling is similar in complexes I and III, a smaller $E_{th}^{\ddagger}$ for complex I means that complex I experiences a greater resonance energy and consequently has more intensity in its IT transition. Finally, asymmetric complex VII, which has both propylene and butylene compartments, was found to be localized in the EPR experiment up to temperatures of 390 K in acetone. The IT band for complex VII can be seen in Figure 12 to be the weakest of these three complexes.

In Figure 13 the spectra for complexes I, IV, and VI are compared. It is interesting that the spectra for the two symmetric complexes, I and IV, are so similar. Complex IV does appear to have a somewhat weaker IT band than is observed for complex I, but a greater difference would have been expected on the basis of the EPR results. It is difficult to identify and calibrate the IT band for asymmetric complex VI. Perhaps the shoulder at 12.1 $\times$ 10$^3$ cm$^{-1}$ is the IT band for this complex.

As reported by Gagné et al.[3], we find that the electronic absorption spectra of the seven Cu$^{II}$Cu$^{I}$ complexes do change somewhat from one solvent to another. Also, in the case of a solvent such as CH$_2$Cl$_2$, spectra could be run to lower energies than 6000 cm$^{-1}$. Complex I shows two apparent IT bands in CH$_2$Cl$_2$, one at 8.62 $\times$ 10$^3$ cm$^{-1}$ ($\epsilon$ 430 M$^{-1}$ cm$^{-1}$) and the other

at $5.75 \times 10^3$ cm$^{-1}$ ($\epsilon$ 310 M$^{-1}$ cm$^{-1}$). Complexes III and IV do not show a second lower energy IT band in CH$_2$Cl$_2$.

## Conclusion and Comments

A series of seven mixed-valence Cu$^{II}$Cu$^{I}$ complexes has been prepared. As characterized by EPR, four of the complexes are delocalized at room temperature in solution and three are localized. Temperatures of transformation from EPR localized to EPR delocalized were found to range from $\sim$200 K for complex I to something in excess of $\sim$390 K for complexes IV, VI, and VII. Data on the IT electronic absorption bands seems to be of less direct use compared to the reported EPR data.

Solomon and co-workers[2] have been able to prepare the "half-met" mixed-valence Cu$^{II}$Cu$^{I}$ state for the binuclear copper active sites in a number of copper proteins. In fact, they have found this half-met mixed-valence state to be the most useful in probing these binuclear copper sites. Electronic absorption and EPR spectra have been used to characterize the mixed-valence sites of the copper proteins. Because there are so few well-characterized binuclear Cu$^{II}$Cu$^{I}$ complexes, the work reported in this paper should help in understanding the data for the copper proteins. One pronounced difference between the properties of our mixed-valence binuclear complexes and those reported for the Cu$^{II}$Cu$^{I}$ protein sites can already be identified. EPR spectra were presented for the mixed-valence copper proteins only at 77 K (not so easy to obtain a room-temperature solution spectrum). Solomon[2] characterizes these EPR signals as being different than those obtained for proteins containing only mononuclear Cu$^{II}$ sites and states that they "exhibit more than four copper parallel hyperfine lines, thus indicating that the unpaired electron is also interacting with the Cu(I)". In contrast, the frozen-glass EPR spectra for our complexes are simple axial spectra with four copper parallel hyperfine lines. The implication from Solomon's work is that the mixed-valence Cu$^{II}$Cu$^{I}$ protein sites are EPR delocalized at 77 K. It would probably take a remarkable binucleating ligand (protein?) to obtain a mixed-valence Cu$^{II}$Cu$^{I}$ site where the frequency of electron exchange between copper sites remains high at very low temperatures.

A few comments contrasting the nature of the present species of Cu$^{II}$Cu$^{I}$ complexes with those of more extensive series of binuclear mixed-valence complexes are in order. The two most thoroughly studied series of binuclear complexes are the mixed-valence ruthenium amine complexes[14] and the mixed-valence biferrocenes.[15] In the PKS vibronic coupling model[13] for such mixed-valence complexes, at least three parameters are needed to describe the properties of the complex. In the case of each symmetric mixed-valence complex, thre are intially two degenerate electronic states, and this degeneracy leads to a coupling of the electronic coordinates to appropraite vibrational coordinates. In analogy to the Jahn–Teller effect,[16] this leads to the well-publicized double-well potential energy diagram for a mixed-valence complex, see Figure 14. In these diagrams, the potential energy of the binuclear complex is plotted as a function of a change in the effective vibrational coordinate that is coupled to the electronic states. Electronic coupling between the two metal centers in the binuclear complex is gauged by the parameter $\epsilon$, whereas the vibronic coupling is gauged by the $\lambda$ parameter in the PKS theory.[13] In the simple case of a centrosymmetric binuclear complex comprised of octahedrally coordinated metal sites, the $\lambda$ parameter is directly proportional to the *difference* in the equilibrium value of the symmetric metal–ligand stretching normal coordinates in the two different oxidation-state monomers. For this discussion we can neglect the third parameter, $W$, in the PKS theory. This is in an electronic parameter that gauges the difference in zero-point energies for the two states of the mixed-valence complex.

In the case of the mixed-valence ruthenium amines and biferrocenes, the bridge or interconnective element between the two metal complexes is varied. Thus, the vibronic coupling parameter $\lambda$ does *not* change appreciably in either of these series, where most of the immediate ligands about the metal are held constant. In these two series, the electronic coupling parameter $\epsilon$ is the main parameter that reflects a change in the bridge. On the other hand, in our series of mixed-valence copper complexes it is likely that the electronic parameter $\epsilon$ is not varying tremendously in the series. Appreciable, but perhaps not dominating, zero-point electronic energy differences ($W$ parameter) would be present for complexes VI and VII. It is likely that the vibronic couling parameter $\lambda$ is influential in controlling the electron dynamics in this Cu$^{II}$Cu$^{I}$ series. A large value of $\lambda$ indicates a considerable difference in the vibrational normal coordinates for the Cu$^{II}$ sites compared to those for the Cu$^{I}$ sites for those vibrational modes that are coupled to the electronic coordinates. It can be seen in Figure 14 that an increase in the value of $\lambda$ effectively increases the barrier height for electron transfer.

## Experimental Section

**Materials.** All solvents were purified before use. Acetone was triply distilled over KMnO$_4$, followed by K$_2$CO$_3$, and then molecular sieves. Dimethylformamide (DMF) was purified by distillation over BaO. The reactant 4-*tert*-butyl-2,6-diformylphenol was synthesized by using a procedure described by Desmond.[17] All diamines were reagent grade and used as received. A sample of 2,2'-diaminobiphenyl was prepared as reported.[18] The reagents CuCO$_3$ and aqueous HBF$_4$ were used to prepare Cu(BF$_4$)$_2$·6H$_2$O. The electrolyte tetrabutylammonium perchlorate (TBAP) was recrystallized five times from ethanol and then dried in vacuo.

**Physical Measurements.** EPR experiments in the range of room to liquid-nitrogen temperature were carried out in a Varian E9 X-band spectrometer equipped with a gas-flow temperature controller. A calibrated copper–constantan thermocouple was used to determine sample temperatures. Liquid-helium EPR work was done on a Bruker ER200 X-band spectrometer. All samples of air-sensitive mixed-valence complexes were loaded in EPR tubes in a Vacuum Atmospheres HE-43-2 glove box charged with an oxygen-free argon atmosphere. Solutions for EPR experiments were loaded in the box and then were degassed and sealed off on a glass vacuum line.

Electronic absorption spectra were measured at room temperature on a Cary 14 spectrophotometer. Solutions of the mixed-valence complexes were prepared in the inert atmosphere box.

**Electrochemistry.** All electrochemical measurements were made with a PAR Model 174 Polarographic Analyzer connected to a X–Y Omnigraphic Model 2000 recorder. Differential pulse polarography and cyclic voltammetry were made in a cell containing a platinum working electrode, auxiliary electrode, and an Ag/AgNO$_3$ in acetonitrile reference electrode with an inert atmosphere. DMF was employed as the solvent for all electrochemical measurements. The oxidation wave for ferrocene ($5 \times 10^{-4}$ M) dissolved in the solution with the complex was used as an internal calibration for voltage measurements. This oxidation wave occurs at 0.400 V vs. the normal hydrogen electrode (NHE) and is considered solvent independent.[19] The concentration of the binuclear copper complexes was in the range of $1 \times 10^{-3}$ to $2.5 \times 10^{-3}$ M.

**Preparation of Complexes.** A simple nomenclature scheme is needed in order to simplify the description of each complex. We will identify the basic binucleating ligand as L followed by the specifics in parentheses of which R$_1$ and R$_2$ diamine linkages are employed. The asymmetric complexes with two different metal sites were made in steps. First, one diamine was condensed with 2 mol of 4-*tert*-butyl-2,6-diformylphenol to give a mononucleating ligand we will label L' with specifics in parentheses.

**Cu$^{II}$Cu$^{II}$L(BF$_4$)$_2$·H$_2$O (R$_1$ = R$_2$ = Propylene).** The diamine 1,3-diaminopropane (0.95 g, 12.8 mmol) dissolved in 15 mL of methanol was added to a flask containing Cu(BF$_4$)$_2$·6H$_2$O (4.29 g, 12.4 mmol) dissolved in 50 mL of methanol. After the solution was warmed, 4-*tert*-butyl-2,6-diformylphenol (2.56 g, 12.4 mmol) was added. The stirred solution was refluxed for 2 h. The solution was then concentrated to 20 mL and cooled. A green precipitate was isolated by filtration and then recrystallized from H$_2$O. Anal. Calcd for Cu$_2$C$_{30}$H$_{40}$N$_4$O$_3$B$_2$F$_8$: Cu, 15.8; C,

(14) (a) Tanner, M.; Ludi, A. *Inorg. Chem.* **1981**, *20*, 2350 and references therein. (b) Citrin, P. H.; Ginsberg, A. P. *J. Am. Chem. Soc.* **1981**, *103*, 3673 and references therein. (c) Creutz, C.; Taube, H. *Ibid.* **1969**, *91*, 3988.

(15) Kramer, J. A.; Herbstein, F. H.; Hendrickson, D. N. *J. Am. Chem. Soc.* **1980**, *102*, 2293. Kramer, J. A.; Hendrickson, D. N. *Inorg. Chem.* **1980**, *19*, 3330 and references therein.

(16) Ammeter, J. H.; Zoller, L.; Bachmann, J.; Baltzer, P.; Gamp, E.; Bucher, R.; Deiss, E. *Helv. Chim. Acta* **1981**, *64*, 1063.

(17) Desmond, M. Ph.D Thesis, University of Illinois, 1979.

(18) Vogel, A. I. "Practical Organic Chemistry", 3rd ed.; Wiley: New York, 1966; p 563.

(19) Bauer, D.; Breant, M. "Electroanalytical Chemistry"; Bard, A. J., Ed.; Marcel Dekker: New York, 1975; Vol. 8, pp 282–344.
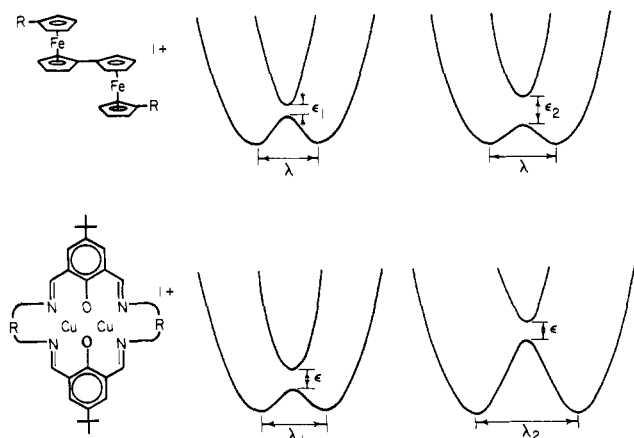
**Figure 14.** Potential energy diagrams for mixed-valence complexes illustrating that a variation in electronic coupling ($\epsilon$) is dominant for the mixed-valence biferrocenes, whereas a variation in vibronic coupling ($\lambda$) is probably important in the mixed-valence copper complexes studied in this work.

44.7; H, 4.8; N, 7.0. Found: Cu, 15.5; C, 44.6; H, 4.7; N, 7.1.

**Cu$^{II}$Cu$^{II}$L(BF$_4$)$_2$·H$_2$O (R$_1$ = R$_2$ = 2,2'-Dimethylpropylene).** An ethanolic solution of 10 mL of 0.626 M 2,2'-dimethyl-1,3 diaminopropane was pipetted into a solution containing Cu(BF$_4$)$_2$·6H$_2$O (2.15 g, 6.2 mmol) dissolved in 30 mL of methanol. After heating this solution, 4-*tert*-butyl-2,6-diformylphenol (1.29 g, 6.3 mmol) dissolved in 30 mL of warm methanol was added. The stirred solution was refluxed for 2 h. The solution was then concentrated to 30 mL and precipitation occurred. The precipitate was recrystallized from hot H$_2$O. Anal. Calcd for Cu$_2$C$_{34}$H$_{48}$N$_4$O$_3$B$_2$F$_8$: Cu, 14.8; C, 47.4; H, 5.6; N, 6.5. Found: Cu, 14.8; C, 47.9; H, 5.4; N, 6.4.

**Cu$^{II}$Cu$^{II}$L(BF$_4$)$_2$ (R$_1$ = R$_2$ = Butylene).** To a solution of Cu(BF$_4$)$_2$·6H$_2$O (4.72 g, 13.7 mmol) dissolved in 40 mL of methanol was added 1,4-diaminobutane (1.5 g, 17.0 mmol) dissolved in 5 mL of methanol. 4-*tert*-Butyl-2,6-diformylphenol (2.82 g, 13.7 mmol) was then added to the solution. The solution mixture was stirred and refluxed under dry air for 3 h. After this, more 1,4-diaminobutane (1.2 g, 13.0 mmol) was added. The solution was refluxed for 5 h more, and then stirred at room temperature for 12 h. The solution was then concentrated under reduced pressure. The resulting precipitate was filtered, washed with methanol and ether, and twice recrystallized from methanol. Anal. Calcd for Cu$_2$C$_{32}$H$_{42}$N$_4$O$_2$B$_2$F$_8$: Cu, 15.6; C, 47.1; H, 5.2; N, 6.9. Found: Cu, 15.7; C, 47.8; H, 6.0; N, 6.9.

**Cu$^{II}$Cu$^{II}$L(BF$_4$)$_2$·CH$_3$OH (R$_1$ = R$_2$ = 2,2'-Biphenylene).** To a solution containing Cu(BF$_4$)$_2$·6H$_2$O (3.25 g, 9.4 mmol) dissolved in 60 mL of methanol was added 2,2'-diaminobiphenyl (1.73 g, 9.4 mmol). After the solution was warmed, 4-*tert*-butyl-2,6-diformylphenol (1.94 g, 9.4 mmol) was added. The solution was heated and stirred for 2 h, after which a precipitate formed. The precipitate was filtered, washed with ether, and then recrystallized from a methanol-water solvent mixture. Anal. Calcd for Cu$_2$C$_{49}$H$_{46}$N$_4$O$_2$B$_2$F$_4$: Cu, 12.2; C, 56.5; H, 4.5; N, 5.4. Found: Cu, 12.2; C, 56.3; H, 4.3; N, 5.4.

**Cu$^{II}$L' (R$_1$ = Propylene).** To a solution of 4-*tert*-butyl-2,6-diformylphenol (1.25 g, 6.1 mmol) dissolved in 40 mL of THF was added dropwise 1,3-diaminopropane (0.23 g, 3.1 mmol). Cu(OAc)$_2$·H$_2$O (0.62 g, 3.1 mmol) was then added, followed by the addition of 10 mL of dichloromethane. The stirred solution was heated for 15 min and then cooled. The resulting precipitate was filtered and washed with methanol. Anal. Calcd for CuC$_{27}$H$_{32}$N$_2$O$_4$: Cu, 11.8; C, 60.8; H, 6.1; N, 5.2. Found: Cu, 11.5; C, 61.1; H, 6.0; N, 4.9.

**Cu$^{II}$Cu$^{II}$L(BF$_4$)$_2$·CH$_3$OH (R$_1$ = Propylene; R$_2$ = 2,2'-Dimethylpropylene).** A quantity of Cu$^{II}$L' (R = propylene) (0.70 g, 1.4 mmol) was added to a solution containing Cu(BF$_4$)$_2$·6H$_2$O (0.48 g, 1.4 mmol) dissolved in 45 mL of warm methanol. The solution was brought to reflux temperature, and then 2.4 mL of an ethanolic 0.65 M 2,2'-dimethyl-1,3-diaminopropane (1.6 mmol) was added. The stirred solution was then refluxed for 2 h. Afterward, the solution was concentrated, cooled, and filtered. The resulting precipitate was washed with H$_2$O, methanol, and then ether. Anal. Calcd for Cu$_2$C$_{33}$H$_{46}$N$_4$O$_2$B$_2$F$_8$: Cu, 15.0; C, 46.8; H, 5.2; N, 6.6. Found: Cu, 14.8; C, 46.4; H, 5.2; N, 6.7.

**Cu$^{II}$Cu$^{II}$L(BF$_4$)$_2$·2CH$_3$OH (R$_1$ = Propylene; R$_2$ = 2,2'-Biphenylene).** To a slurry of Cu$^{II}$L' (R$_1$ = propylene) (2.55 g, 5.0 mmol) in 30 mL of methanol was added Cu(BF$_4$)$_2$·6H$_2$O (1.72 g, 5.0 mmol) dissolved in 15 mL of methanol. Then 2,2'-diaminobiphenyl (0.92 g, 5.1 mmol) dissolved in 15 mL of methanol was added, and the stirred solution was heated

gently for 4 h. The solution was then concentrated under reduced pressure and cooled. The resulting precipitate was filtered and washed with methanol. The precipitate was recrystallized from methanol. Anal. Calcd for Cu$_2$C$_4$H$_{48}$N$_4$O$_4$B$_2$F$_8$: Cu, 13.2; C, 51.2; H, 5.0; N, 5.8. Found: Cu, 13.3; C, 49.9; H, 4.9; N, 5.9.

**Cu$^{II}$Cu$^{II}$L(BF$_4$)$_2$ (R$_1$ = Propylene; R$_2$ = Butylene).** A sample of Cu$^{II}$L' (R$_1$ = propylene) (1.27 g, 2.5 mmol) was suspended in 50 mL of methanol. Cu(BF$_4$)$_2$·6H$_2$O (0.855 g, 2.5 mmol) dissolved in 10 mL of methanol was added followed by the addition of 1,4-diaminobutane (0.30 g, 3.4 mmol) dissolved in 5 mL of methanol. The reaction mixture was stirred and refluxed for 16 h under dry air. The solution was concentrated under reduced pressure and then cooled. The resulting precipitate was filtered and washed with methanol and a large amount of ether. The precipitate was recrystallized from a large quantity of a methanol-H$_2$O (1:10) solvent mixture. Anal. Calcd for Cu$_2$C$_{31}$H$_{40}$N$_4$O$_2$B$_2$F$_8$: Cu, 15.9; C, 46.7; H, 5.1; N, 7.0. Found: Cu, 15.8; C, 46.3; H, 5.3; N, 7.3.

**Cu$^{II}$Cu$^{I}$L(BF$_4$)·0.5CH$_3$OH (R$_1$ = R$_2$ = Butylene).** A sample of the corresponding Cu$^{II}$Cu$^{II}$L complex (0.42 g, 0.5 mmol) was dissolved in 50 mL of methanol. Some 2.1 mL of 0.5 M NaOH (aq) (1.1 mmol) was added, and the resulting reaction mixture was degassed. Na$_2$S$_2$O$_4$ (0.045 g, 0.25 mmol) dissolved in 25 mL of degassed H$_2$O was added to the reaction mixture with syringe techniques. A dark brown precipitate formed upon addition of the Na$_2$S$_2$O$_4$ solution and reduced pressure. The precipitate was isolated by filtration with Schlenkware techniques and transferred to the argon atmosphere of the dry box. Anal. Calcd for Cu$_2$C$_{32.5}$H$_{44}$N$_4$O$_{2.5}$BF$_4$: Cu, 17.1; C, 52.4; H, 6.0; N, 7.5. Found: Cu, 17.0; C, 52.4; H, 5.9; N, 7.5.

Samples of the tetrafluoroborate salts of the other six mixed-valence Cu$^{II}$Cu$^{I}$ complexes were prepared in the same manner as indicated above for the butylene complex III. Analytical data follow.

**Complex I·(CH$_3$OH):** Calcd for Cu$_2$C$_{31}$H$_{42}$N$_4$O$_3$BF$_4$: Cu, 17.4; C, 50.8; H, 5.8; N, 7.6. Found: Cu, 17.6; C, 50.4; H, 5.5; N, 7.4.

**Complex II:** Calcd for Cu$_2$C$_{34}$H$_{46}$N$_4$O$_2$BF$_4$: Cu, 16.8; C, 54.0; H, 6.1; N, 7.4. Found: Cu, 16.9; C, 53.8; H, 6.2; N, 7.2.

**Complex IV:** Calcd for Cu$_2$C$_{48}$H$_{42}$N$_4$O$_2$BF$_4$: Cu, 13.8; C, 62.6; H, 4.6; N, 6.1. Found: Cu, 13.4; C, 62.8; H, 4.8; N, 6.0.

**Complex V:** Calcd for Cu$_2$C$_{32}$H$_{42}$N$_4$O$_2$BF$_4$: Cu, 17.4; C, 52.7; H, 5.8; N, 7.7. Found: Cu, 17.5; C, 52.2; H, 5.7; N, 7.5.

**Complex VI·(CH$_3$OH):** Calcd for Cu$_2$C$_{40}$H$_{44}$N$_4$O$_3$BF$_4$: Cu, 15.1; C, 57.0; H, 5.3; N, 6.7. Found: Cu, 14.7; C, 56.9; H, 5.1; N, 6.9.

**Complex VII·(CH$_3$OH):** Calcd for Cu$_2$C$_{32}$H$_{44}$N$_4$O$_3$BF$_4$: Cu, 17.0; C, 51.5; H, 5.9; N, 7.5. Found: Cu, 16.8; C, 51.3; H, 5.7; N, 7.6.

**Cu$^{II}$Cu$^{II}$L(BPh$_4$)$_2$·2((CH$_3$)$_2$CO) (R$_1$ = R$_2$ = 2,2'-Dimethylpropylene).** A quantity (0.68 g, 0.8 mmol) of the corresponding BF$_4^-$ salt was dissolved in 115 mL of methanol-H$_2$O (4:3). Some NaBPh$_4$ (1 g, 3 mmol) was then added. A precipitate formed immediately upon addition of NaBPh$_4$. The precipitate was filtered and washed with methanol and ether and recrystallized from acetone-H$_2$O. Anal. Calcd for Cu$_2$C$_{88}$H$_{98}$N$_4$B$_2$O$_4$: Cu, 8.9; C, 74.2; H, 6.9; N, 3.9. Found: Cu, 8.6; C, 74.0; H, 7.3; N, 3.9.

**Cu$^{II}$Cu$^{I}$L(BPh$_4$)·((CH$_3$)$_2$CO) (R$_1$ = R$_2$ = 2,2'-Dimethylpropylene).** The BPh$_4^-$ salt of the corresponding Cu$^{II}$Cu$^{II}$ compound (0.34 g, 0.24 mmol) was dissolved in 30 mL of acetone. A 1.1-mL sample of 0.5 M NaOH (aq) (0.55 mmol) was added to the solution, which was then degassed. Na$_2$S$_2$O$_4$ (0.023 g, 0.13 mmol) dissolved in 15 mL of degassed H$_2$O was added with syringe techniques. A precipitate formed immediately and was isolated with Schlenkware techniques and transferred to the argon-atmosphere dry box. Anal. Calcd for Cu$_2$C$_{61}$H$_{72}$N$_4$BO$_3$: Cu, 12.1; C, 70.0; H, 6.9; N, 5.4. Found: Cu, 12.0;, C, 70.1; H, 6.8; N, 5.4.

**Registry No.** I, 84501-16-6; II, 84501-18-8; III, 84501-14-4; IV, 84501-20-2; V, 84501-22-4; VI, 84520-66-1; VIII, 84501-24-6; Cu$^{II}$-Cu$^{II}$L(BF$_4$)$_2$ (R$_1$ = R$_2$ = propylene), 84520-62-7; Cu$^{II}$Cu$^{II}$L(BF$_4$)$_2$ (R$_1$ = R$_2$ = 2,2-dimethylpropylene), 84520-60-5; Cu$^{II}$Cu$^{II}$L(BF$_4$)$_2$ (R$_1$ = R$_2$ = butylene), 84520-64-9; Cu$^{II}$Cu$^{II}$L(BF$_4$)$_2$ (R$_1$ = R$_2$ = 2,2'-biphenylene), 84520-59-2; Cu$^{II}$L' (R$_1$ = propylene), 84501-10-0; Cu$^{II}$Cu$^{II}$L(BF$_4$)$_2$ (R$_1$ = propylene; R$_2$ = 2,2-dimethylpropylene), 84520-57-0; Cu$^{II}$Cu$^{II}$L(BF$_4$)$_2$ (R$_1$ = propylene; R$_2$ = 2,2'-biphenylene), 84520-55-8; Cu$^{II}$Cu$^{II}$L(BF$_4$)$_2$ (R$_1$ = propylene; R$_2$ = butylene), 84501-12-2; Cu$^{II}$Cu$^{II}$L(BPh$_4$)$_2$ (R$_1$ = R$_2$ = 2,2-dimethylpropylene), 84501-26-8; Cu$^{II}$Cu$^{I}$L(BPh$_4$)$_2$ (R$_1$ = R$_2$ = 2,2-dimethylpropylene), 84501-27-9; 1,3-diaminopropane, 109-76-2; 2,2-dimethyl-1,3-diaminopropane, 7328-91-8; 1,4-diaminobutane, 110-60-1; 2,2'-diaminobiphenyl, 1454-80-4; 4-*tert*-butyl-2,6-diformylphenol, 84501-28-0.

**Supplementary Material Available:** Figures 5 and 10 are available (2 pages). Ordering information is given on any current masthead page.